Jurnal Polimesin
Department of Mechanical Engineering
State Polytechnic of Lhokseumawe
http://e-jurnal.pnl.ac.id/polimesin
e-ISSN : 2549-1999 No. : 2 Month : April
p-ISSN : 1693-5462 Volume : 24 Year : 2026

Processing dates: received on 2026-1-27, reviewed on 2026-03-29, accepted on 2026-04-02 and online availability on 2026-04-25

Experimental investigation of wear-hardness trade-off mapping for quenched HSS tools under different quenching media and austenitizing temperatures

Razali*, Reinaldi Teguh Setyawan, Alfazan Yendra
Department Mechanical Engineering, Politeknik Negeri Bengkalis, Bengkalis 28712, Indonesia
*Corresponding author: razali@polbeng.ac.id

Abstract

This study investigates the wear-hardness trade-off of quenched AISI M2 High-Speed Steel (HSS) cutting tools subjected to three austenitizing temperatures (800, 900, and 1000°C) and three quenching media (salt water, Bromus oil, and SAE 20 oil), without subsequent tempering treatment. A factorial dataset consisting of three austenitizing temperatures (800, 900, and 1000°C) and three quenching media (salt water, Bromus oil, and SAE 20 oil) was analyzed under fixed turning parameters ($n = 300$ rpm, $f = 0.19$ mm/rev, $a_p = 1.5$ mm). Tool performance was evaluated using flank wear (VB) and Rockwell hardness (HRC), with five hardness readings per condition to quantify repeatability. The results show a dominant temperature effect: VB decreases monotonically as austenitizing temperature increases, while hardness rises markedly at 1000°C, forming a favorable region with simultaneously low wear and high hardness. The best combined performance was obtained at 1000°C with SAE 20 oil, achieving VB = 0.066 mm and HRC ≈ 82.8. A desirability-style composite index D, derived from normalized VB (smaller-is-better) and HRC (larger-is-better), produced decision and rank maps that consistently identified the 1000°C region as the optimal operating window, with oil quenching preferred when high-temperature austenitizing is feasible. Hardness repeatability metrics further indicated that the 1000°C conditions exhibit the lowest scatter, strengthening their practical robustness. The proposed mapping framework offers a compact, reproducible approach to visualize the wear–hardness trade-off and to rank heat-treatment conditions using existing experimental data.

Keywords:
High-speed steel, quenching media, heat map mapping, trade-off analysis, austenitizing temperature.

1 Introduction

High-Speed Steel (HSS) cutting tools remain widely used in turning operations where affordability, regrindability, and practical robustness are required. In many workshop-scale and educational machining settings, HSS continues to be a relevant tooling option for moderate cutting conditions and flexible maintenance [1]. Under such circumstances, tool performance is commonly evaluated by progressive wear at the cutting edge, as it directly influences dimensional accuracy, surface integrity, and process stability [2].

A key wear indicator in turning is flank wear (VB), which represents material loss along the tool flank in contact with the newly machined surface. Increasing VB is generally associated with rising cutting forces, loss of dimensional control, and deterioration of surface finish [3]. Nevertheless, wear metrics alone may not fully describe tool reliability. In practice, a tool may exhibit favorable wear behavior yet still suffer from premature edge damage, such as micro-chipping, when the tool material condition becomes excessively brittle or when residual stresses are unfavorable. Therefore, engineering decisions on HSS tool preparation benefit from considering wear together with a material-property indicator that reflects the tool's resistance to deformation and its ability to sustain cutting loads [4].

The final material state of HSS is strongly affected by heat treatment, particularly the selection of austenitizing temperature and quenching medium. Austenitizing temperature influences carbide dissolution and alloying element distribution in austenite, while the quenching medium governs cooling severity and thermal gradients that control transformation behavior and residual stress development [5]. In HSS tools, the final mechanical response after quenching is governed not only by nominal hardness, but also by the resulting microstructural condition. Austenitizing controls the extent of carbide dissolution and the enrichment of austenite with carbon and alloying elements. At the same time, quenching determines the transformation path toward a hardened martensitic structure together with possible retained austenite, undissolved carbides, and quenching-induced residual stresses. These microstructural features directly influence the balance between wear resistance, edge stability, and brittleness during cutting. In conventional tool-steel practice, tempering is commonly applied after quenching to relieve internal stresses, improve dimensional stability, and partially restore toughness lost during severe hardening. However, the present study focuses on the as-quenched response without subsequent tempering to isolate the combined influence of austenitizing temperature and quenching medium on the observed wear-hardness behavior. Accordingly, the metallurgical interpretations developed in this work are limited to the as-quenched condition within the tested turning regime. These parameters may generate competing effects: conditions that promote higher hardness can enhance resistance to abrasive and adhesive wear, but the same conditions can also increase brittleness and stress-driven damage susceptibility at the cutting edge. This inherent competition gives rise to a wear–hardness trade-off that should be explicitly evaluated for rational selection of heat-treatment parameters [6].

Hardness is commonly measured on the Rockwell C scale (HRC) for tool steels due to its standardized and efficient measurement. Higher HRC generally indicates increased resistance to plastic deformation and can be associated with improved wear resistance [7]. However, hardness improvement does not automatically translate to superior cutting performance if the increase is accompanied by reduced toughness or elevated residual stresses. Consequently, interpreting VB and HRC jointly is more informative than assessing either response in isolation, particularly when the objective is to identify practical heat-treatment settings that deliver stable cutting performance [8].

Existing reports often communicate heat-treatment outcomes through separate plots or tables for wear and hardness, followed by single-response ranking. While this approach is straightforward, it can obscure the combined interpretation needed for decision-making across multiple parameter combinations [9]. Specifically, it becomes difficult to visualize how wear reduction aligns with hardness evolution over the entire parameter space and to identify balanced regions where low wear is achieved without compromising hardness-related reliability [10]. A compact mapping approach that preserves the factorial structure of the tested conditions can improve interpretability and strengthen recommendations for practical use.

To address this limitation, this study proposes a heatmap-based performance-mapping framework to analyze the wear–hardness trade-off of quenched HSS tools across combinations of quenching media and austenitizing temperatures under constant turning conditions [11]. In the proposed approach, VB is visualized as a

performance heatmap, and HRC information is integrated to reveal trade-offs across all tested conditions in a single, decision-oriented representation. In addition, multiple hardness readings per condition are exploited to quantify hardness repeatability, supporting a more robust interpretation of the mapped trends. Finally, an explicit composite performance index is formulated to provide a transparent ranking of conditions with the dual objective of minimizing VB and maximizing HRC [12].

Accordingly, the objective of this paper is to develop and demonstrate an integrated wear–hardness trade-off mapping method for selecting quenching conditions for HSS tools [13]. The main contributions include (1) heatmap-based visualization of VB across the parameter matrix, (2) integrated interpretation of VB and HRC to highlight trade-offs, (3) repeatability-aware hardness reporting using multiple readings per condition, and (4) a composite decision map that supports practical selection of quenching settings. The remainder of the paper presents the mapping methodology, results, discussion of observed trends, and concluding recommendations.

From a methodological standpoint, the present study is not intended as a full predictive multi-response optimization model. Although multi-response decision strategies such as desirability analysis, response-surface-based optimization, and factor-significance evaluation are widely used in manufacturing studies, their practical application is often oriented toward formal process optimization with larger experimental programs and model-based parameter estimation. In contrast, the present work is positioned as a compact decision-mapping approach for a small factorial heat-treatment dataset, where the main need is not extensive optimization but transparent interpretation of the wear–hardness trade-off across tested conditions [13]. The methodological contribution, therefore, lies in integrating three elements within a single framework: (1) matrix-preserving heatmap visualization of flank wear across the full treatment space, (2) repeatability-aware hardness interpretation using SD, CV, and confidence intervals, and (3) a desirability-style composite ranking used as a transparent decision aid rather than as a full predictive optimization model. This positioning distinguishes the study from conventional single-response comparisons and broader optimization studies by emphasizing interpretability, reproducibility, and direct engineering selection of quenching conditions from existing experimental data.

2 Research methodology

This study applies a structured, data-driven mapping approach to evaluate the wear–hardness trade-off of quenched HSS cutting tools. The methodology is designed to (1) preserve the factorial structure of the available dataset, (2) visualize flank wear (VB) and Rockwell hardness (HRC) in an integrated manner, and (3) support decision-making through a transparent composite performance index. The overall workflow consists of: data assembly into response matrices, hardness repeatability quantification, heatmap-based performance mapping, composite-index formulation, and condition ranking. Methodologically, this study should be viewed as a decision-oriented mapping framework for factorial experimental data, rather than a full predictive multi-objective optimization model.

2.1 Study design and dataset organization

A factorial framework is adopted based on two controllable heat-treatment factors: austenitizing temperature and quenching medium. Austenitizing temperature is considered at three levels (800°C, 900°C, 1000°C), while the quenching medium is categorized into three types (salt water, Bromus oil, SAE 20 oil). This forms a 3×3 experimental matrix (nine heat-treatment conditions). The turning (machining) parameters are maintained constant to ensure that differences in tool performance are primarily attributed to heat-treatment settings rather than machining variability.

The cutting tools used in this study were commercial HSS single-point turning tools with nominal dimensions of 12 mm × 12 mm × 100 mm. The tool geometry was prepared with a back rake angle of 8°, side rake angle of 12°, end relief angle of 6°, side relief angle of 6°, end cutting edge angle of 8°, side cutting edge angle of 15°, and nose radius of 0.8 mm. Heat treatment was performed in an electric resistance muffle furnace at three austenitizing temperatures; 800, 900, and 1000°C. Each specimen was held at the target temperature for 30 min before quenching. After soaking, the tools were immediately quenched in one of three media: salt water, Bromus oil, or SAE 20 oil. The quenching media were maintained near room temperature, approximately 28 ± 2°C for salt water and 30 ± 2°C for both oil media. The transfer time from the furnace to the quenching bath was controlled within approximately 2–3 s. Mild agitation was applied during the initial 3–5 s of immersion to reduce local temperature non-uniformity, after which the tool remained immersed until it approached room temperature. No tempering treatment was applied after quenching.

The dataset is arranged into two aligned matrices: one matrix for VB and another for HRC [14]. Each cell corresponds to one unique combination of temperature and quenching medium. This structure enables direct comparison across temperature levels (row-wise) and quenching media (column-wise), which is essential for mapping-based interpretation.

Table 1 summarizes the experimental framework used in this study. Austenitizing temperature (Ta) was set at 800, 900, and 1000°C, and three quenching media (Qm) were considered, namely salt water, Bromus oil, and SAE 20 oil, forming a 3×3 condition matrix [15]. The HSS tools were heat-treated in an electric resistance muffle furnace with a soaking time of 30 min at the selected temperature, followed by immediate quenching with a transfer time of approximately 2–3 s. To isolate the effect of heat treatment, the turning parameters were kept constant at n = 300 rpm, f = 0.19 mm/rev, and ap = 1.5 mm. Tool performance was evaluated using flank wear (VB, mm) and Rockwell hardness (HRC), with five hardness readings collected for each condition to support repeatability analysis.

Table 1. Experimental factors, fixed turning conditions, and responses

Item	Levels/setting
Austenitizing temperature, T_a (°C)	800, 900, 1000
Quenching medium, (Q_m)	Salt water; Bromus oil; SAE 20 oil
Turning conditions	n = 300 rpm; f = 0.19 mm/rev; a_p = 1.5 mm
Responses	Flank wear (VB) (mm); hardness HRC (–)
Hardness readings	(N=5) per condition

2.2 Turning conditions and response definitions

Turning trials were conducted on a conventional centre lathe under fixed machining conditions of spindle speed n = 300 rpm, feed f = 0.19 mm/rev, and depth of cut a_p = 1.5 mm. The workpiece material was a low-carbon steel bar with an approximate diameter of 25 mm and a length of 300 mm. Each heat-treatment condition was tested over an effective cutting length of 300 mm, corresponding to approximately 5.3 min of cutting time under the selected spindle speed and feed [16]. The machining conditions were maintained constant for all tool specimens, allowing the resulting differences in wear behavior to be attributed primarily to the heat-treatment variables.

Flank wear (VB) was used as the primary indicator of tool wear, representing progressive material loss on the tool flank surface after turning. In this study, VB was defined as the average flank wear width (VBB), measured at three measurement points along the flank wear land and reported in millimeters. VB was measured using optical microscopy after the turning test for each tool condition. In parallel, Rockwell hardness (HRC) was used to represent the post-quenching material state of the HSS tool [17]. Hardness was measured using the Rockwell C scale with a diamond cone indenter and a 150 kgf major load. For each heat-

treatment condition, five hardness readings were taken and then summarized statistically using the mean, Standard Deviation (SD), Coefficient of Variation (CV), and 95% Confidence Interval (CI).

Table 2 defines the response variables and their measurement basis used in this study. Flank wear (VB) represents the average post-turning wear land width on the tool flank, while Rockwell hardness (HRC) characterizes the hardness state of the quenched HSS tool. These response definitions provide the experimental basis for the subsequent repeatability analysis of hardness readings and the heatmap-based wear–hardness trade-off mapping.

Table 2. Response definitions and measurement descriptions

Response	Symbol	Unit	Measurement description
Flank wear	VB	mm	Measured on the tool flank after turning using optical microscopy. VB was defined as the average flank wear width (VBB), determined from three measurement points along the wear land and reported in millimeters.
Rockwell hardness (C scale)	HRC	–	Measured on the quenched HSS tool using the Rockwell C scale with a diamond cone indenter and 150 kgf major load. Five readings were taken for each condition, and the data were statistically summarized.

2.3 Hardness, repeatability and measurement uncertainty

Hardness measurements inherently include within-condition scatter due to surface preparation, microstructural heterogeneity, and instrument sensitivity. To provide a reliability-aware interpretation, each heat-treatment condition includes multiple hardness readings (n = 5) [18]. Instead of relying solely on the mean HRC, this study quantifies hardness repeatability using descriptive and inferential statistics.

For each condition, the mean hardness ($H\bar{R}C$) is calculated along with the SD and CV. SD characterizes the absolute dispersion of repeated readings, while CV normalizes dispersion relative to the mean [19]. To provide an uncertainty band for the average hardness at each condition, a 95% CI half-width is computed using the Student's t distribution. These metrics allow the analysis to differentiate between conditions that achieve high hardness consistently and conditions that exhibit high hardness with large scatter, which is important when translating laboratory findings into practical recommendations.

Let h_i denote the i^{th} Rockwell hardness reading (HRC) for a given condition, with $i = 1,2,\dots,N$ (Eq. (1)).

$$\text{HRC} = \frac{1}{N}\sum_{i=1}^{N} h_i \tag{1}$$

The SD quantifies the dispersion of repeated hardness readings around the mean (i.e., the absolute scatter in HRC units) (Eq. (2)).

$$\text{SD} = \sqrt{\frac{1}{N-1}\sum_{i=1}^{N}(h_i - HRC)^2} \tag{2}$$

The CV expresses the scatter relative to the mean, reported as a percentage (useful to compare repeatability across conditions with different mean hardness) (Eq. (3)).

$$\text{CV}\ (\%) = \frac{SD}{HRC} \times 100\% \tag{3}$$

A 95% CI for the mean hardness is calculated using the Student's t-distribution (Eq. (4)), where $t_{0.975,\,N-1}$ is the two-sided t-critical value for a 95% confidence level with $N-1$ degrees of freedom. For reporting convenience, the CI half-width can be written as Eq. (5).

$$CI_{95\%}: \text{HRC} \pm \text{t}_{\,0.975,\,\text{N-1}}\left(\frac{SD}{\sqrt{N}}\right) \tag{4}$$

$$CI_{95\%,half} = \text{t}_{\,0.975,\,\text{N-1}}\left(\frac{SD}{\sqrt{N}}\right) \tag{5}$$

2.4 Statistical validation

To strengthen the study's analytical rigor, formal statistical validation was applied to the Rockwell hardness (HRC) data. Since five hardness readings were collected for each treatment condition, the HRC dataset was analyzed using a two-factor Analysis of Variance (two-way ANOVA), with austenitizing temperature (800, 900, and 1000°C) and quenching medium (salt water, Bromus oil, and SAE 20 oil) as fixed factors. The interaction between the two factors was also examined. Prior to ANOVA, the assumptions of residual normality and homogeneity of variance were evaluated using standard diagnostic tests. When statistically significant effects were detected, post-hoc multiple comparison analysis was employed to identify pairwise differences between factor levels.

In contrast, the flank wear (VB) dataset contained one observed value for each treatment combination under fixed turning conditions. Therefore, VB was not subjected to inferential factorial testing in order to avoid unsupported significance claims from non-replicated wear observations. Instead, VB was analyzed descriptively by direct comparison across the factorial matrix and then jointly interpreted with HRC in the integrated performance mapping and composite decision index.

2.5 Composite performance index formulation for trade-off quantification

While integrated heatmaps provide visual insight, a decision-oriented selection of quenching conditions benefits from a single composite metric that combines VB and HRC. The composite index in this study is constructed using a desirability-style normalization so that both responses are transformed onto a comparable 0–1 scale.

Because VB is a "smaller-is-better" response, it is normalized such that lower VB yields a higher desirability score. Conversely, HRC is a "larger-is-better" response, normalized such that higher HRC yields a higher desirability score. The two normalized scores are then combined into a composite index D using a weighted geometric formulation [20]. Equal weighting is adopted when there is no strong preference exists between wear reduction and hardness increase, although the method remains flexible for alternative weighting schemes depending on application priorities.

2.6 Decision mapping and ranking of quenching conditions

After computing the composite index D for all nine conditions, a composite heatmap is generated to form a decision map. This map ranks each temperature–medium combination based on its combined ability to minimize wear and maximize hardness. The best condition is identified as the one with the maximum D, and the ranking is reported alongside the original VB and HRC values to maintain transparency between the raw responses and the final decision.

This decision map is intended to support the practical selection of quenching conditions, especially when engineers require a clear justification for choosing one condition over another in terms of both machining performance and material property outcomes.

2.7 Data processing and implementation

All calculations and visualizations are implemented using MATLAB. The processing steps include: assembling VB and HRC matrices, computing hardness repeatability statistics, performing response normalization, generating VB heatmaps with HRC overlays, computing the composite index D, and producing the composite decision map. This implementation is designed to be fully reproducible, enabling other researchers to apply the same mapping procedure to similar factorial datasets.

2.8 Data consistency check and reporting transparency

To strengthen reproducibility and reporting transparency, a consistency check is applied to hardness data whenever both raw readings and reported averages are available. Specifically, the mean computed from the five raw HRC readings is compared with the

reported average [21]. If a discrepancy exceeds a defined tolerance, it is documented and the analysis prioritizes the mean derived from the raw readings for repeatability calculations. This step ensures that the repeatability metrics are grounded in the measurement-level data and reduces the risk of propagating transcription or reporting inconsistencies.

3 Results and discussion

3.1 Flank wear response across quenching conditions

The flank wear results (VB) show a clear dependence on austenitizing temperature and, to a lesser extent, quenching medium. The highest wear occurred at 800°C with salt water (VB = 0.353 mm), whereas the lowest wear was obtained at 1000°C with SAE 20 oil (VB = 0.066 mm). This corresponds to an overall wear reduction of ≈81.3% from the worst to the best condition.

Fig. 1 provides an integrated view of the wear–hardness response of quenched HSS tools as a function of austenitizing temperature and quenching medium. Across all three quenching media, increasing austenitizing temperature consistently reduced VB: (1) salt water: VB decreased from 0.353 (800°C) → 0.146 (900°C) → 0.080 (1000°C), i.e., ≈ 77.3% reduction from 800°C to 1000°C; (2) Bromus oil: VB decreased from 0.266 → 0.120 → 0.073, i.e., ≈ 72.6% reduction from 800°C to 1000°C; (3) SAE 20 oil: VB decreased from 0.213 → 0.106 → 0.066, i.e., ≈ 69.0% reduction from 800°C to 1000°C.

At 800°C and 900°C, the quenching medium effect is evident: oils (Bromus and SAE 20) produce lower VB than salt water at the same temperature. At 1000°C, the differences between media become smaller (0.066–0.080 mm), suggesting that the austenitizing temperature dominates the wear response in the highest-temperature region.

The monotonic VB reduction with increasing austenitizing temperature indicates that the heat-treatment condition strongly influences the final state of the tool material, which is relevant to wear resistance. From a metallurgical standpoint, the monotonic reduction in VB with increasing austenitizing temperature can be interpreted as a consequence of progressively more effective austenitization prior to quenching. At the lower temperature level of 800°C, carbide dissolution is likely limited, so the austenite formed before quenching may contain less dissolved carbon and alloying elements. This condition would reduce the hardenability of the tool and limit the formation of a sufficiently hard martensitic matrix after cooling, consistent with the higher wear observed at 800°C. When the austenitizing temperature is increased to 900°C and especially to 1000°C, a greater fraction of carbides can dissolve into the austenite, increasing supersaturation before quenching and promoting the formation of a harder transformed structure after cooling. Under turning contact, this harder matrix is more resistant to flank wear, so the progressive decrease in VB with temperature is metallurgically reasonable.

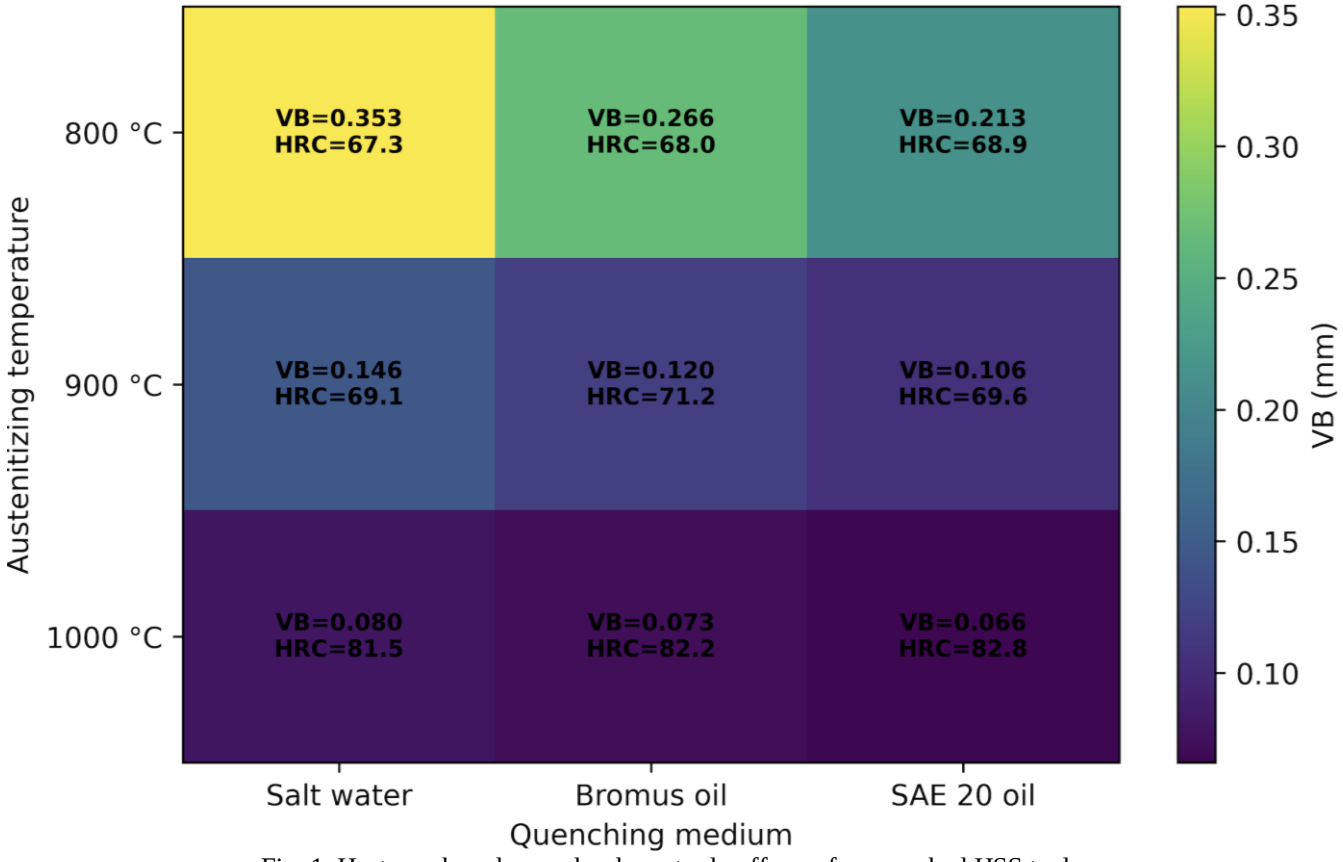

Fig. 1. Heatmap-based wear–hardness trade-off map for quenched HSS tools.

The effect of quenching medium can also be interpreted in terms of cooling severity and thermal-stress development. Salt water is expected to provide the most severe cooling, whereas Bromus oil and SAE 20 oil provide a milder quench. Although severe cooling can promote hardening, it can also increase thermal gradients, residual stresses, and local edge instability, particularly in the absence of tempering. This may explain why, at 800–900°C, oil-quenched tools generally showed lower VB than salt-water-quenched tools even when the hardness levels were not dramatically different. In other words, the wear response in the present dataset appears to depend not only on nominal hardness, but also on the quenching route's influence on the mechanical stability of the cutting edge.

3.2 Hardness (HRC) and repeatability of measurements

Hardness after quenching generally increases with austenitizing temperature, with a marked jump at 1000°C. Using the mean computed from the five repeated readings per condition, the average HRC level rises from approximately 68.1 (800°C) to 70.0 (900°C), then to 82.2 (1000°C) when averaged across the three media.

Because each condition contains five hardness readings, repeatability can be quantified. The most consistent hardness readings (low scatter) were observed at 1000°C, where the SD is below 1 HRC unit for all three media (approximately 0.50–0.76) [22]. In contrast, at 900°C, the scatter is notably larger for salt water (SD ≈ 3.71) and SAE 20 oil (SD ≈ 3.85), which also yields

higher CV values (≈ 5–6%). Such scatter indicates greater within-condition variability or potential sensitivity to measurement location/surface condition at those settings.

Table 3 reports the repeatability of Rockwell hardness (HRC) after quenching based on five readings per condition [23]. Overall, hardness scatter is smallest at 1000°C for all quenching media, as indicated by low SD (≈ 0.50–0.76 HRC) and low CV (≈ 0.61–0.92%), suggesting a more uniform hardness state and more consistent measurement response at the highest austenitizing temperature. In contrast, the 900°C conditions exhibit noticeably larger dispersion for salt water and SAE 20 oil (SD ≈ 3.71–3.85; CV ≈ 5.38–5.53%), implying greater within-condition variability that may arise from local microstructural heterogeneity, surface-condition effects, or quenching sensitivity at that temperature range [24] [25]. The Bromus oil condition at 900°C remains comparatively stable (SD ≈ 1.25; CV ≈ 1.76%), indicating better hardness consistency among the 900°C treatments. These repeatability results are important for interpreting the wear–hardness maps: conditions with similar mean HRC can differ in reliability, and the high-temperature (1000°C) region not only yields higher hardness but also provides a more consistent hardness response, strengthening its suitability for practical quenching parameter selection.

Table 3. Repeatability statistics of Rockwell hardness after quenching (n = 5)

Austenitizing temperature (°C)	Quenching medium	HRC mean	SD	CV (%)	95% CI half-width
800	Salt water	67.3	1.04	1.54	1.29
800	Bromus oil	68.0	0.35	0.52	0.44
80	SAE 20 oil	68.9	1.34	1.95	1.67
900	Salt water	69.1	3.71	5.38	4.61
900	Bromus oil	71.2	1.25	1.76	1.56
900	SAE 20 oil	69.6	3.85	5.53	4.78
1000	Salt water	81.5	0.50	0.61	0.62
1000	Bromus oil	82.2	0.76	0.92	0.94
1000	SAE 20 oil	82.8	0.57	0.69	0.71

3.3 Statistical validation of hardness data

To formally verify the observed hardness trends, a two-way ANOVA was performed on the HRC data using austenitizing temperature and quenching medium as the main factors. The analysis showed that the effect of austenitizing temperature was highly significant on HRC ($F = 230.41$, $p < 0.001$), while the effect of quenching medium was not statistically significant ($F = 1.74$, $p = 0.191$) [26] [27]. The interaction between temperature and quenching medium was not significant ($F = 0.62$, $p = 0.650$), indicating that the hardness response was governed primarily by austenitizing temperature rather than by medium-specific interactions.

These statistical findings support the descriptive hardness patterns shown in the response matrix and repeatability metrics. In practical terms, the ANOVA results confirm that the variation in HRC is not merely due to reading fluctuation, but is systematically associated with the heat-treatment factors investigated in this study. This strengthens the interpretation that the thermal treatment conditions exert a measurable influence on the final hardness of the HSS tools (Tabel 4).

Table 4. Two-way ANOVA summary for HRC

Source	df	SS	MS	F	p-value
Austenitizing temperature	2	1756.300	878.150	230.410	< 0.001
Quenching medium	2	13.233	6.617	1.736	0.191
Temperature × medium	4	9.467	2.367	0.621	0.650
Error	36	137.205	3.811	–	–
Total	44	1916.205	–	–	–

Statistically, these results indicate that hardness development in the present dataset is dominated by austenitizing temperature. Although the quenching media produced small differences in mean HRC at the same temperature, these differences were not strong enough to be statistically separated under the present experimental design. Likewise, the non-significant interaction suggests that the temperature effect remained consistent across the three quenching media.

3.4 Wear–hardness relationship and trade-off behavior

A negative association between hardness and wear is observed across the nine conditions. When VB is plotted against the computed mean HRC values, the Pearson correlation is $r \approx -0.74$, indicating that higher hardness tends to coincide with lower flank wear under the fixed turning conditions. Because the VB dataset consisted of one measured value per treatment condition, the wear results are interpreted descriptively rather than inferentially. Accordingly, the observed VB trends are used as comparative engineering evidence within the factorial mapping framework, while formal statistical significance is reserved for the replicated HRC dataset.

Fig. 2 illustrates the relationship between tool hardness after quenching (HRC) and flank wear (VB) across the nine heat-treatment conditions.

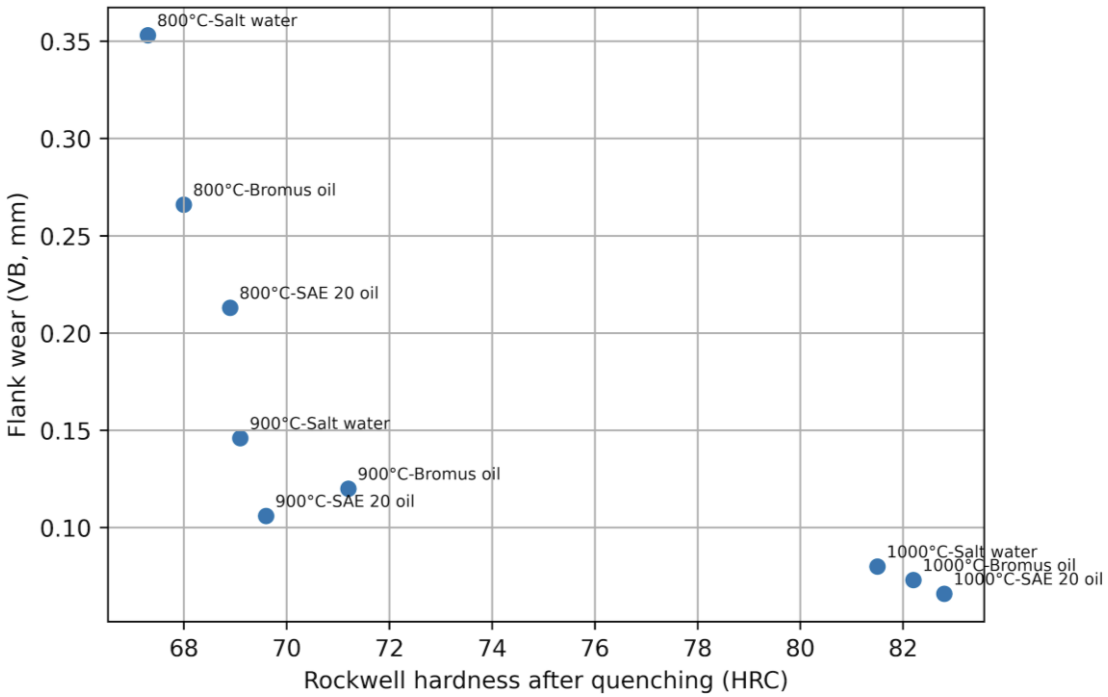

Fig. 2. VB–HRC trade-off scatter plot across quenching conditions for HSS tools.

A clear inverse trend is observed: higher HRC is generally associated with lower VB, with a Pearson correlation of approximately r = −0.743 for the dataset. The 1000°C conditions cluster in the high-hardness/low-wear region (HRC ≈ 81.5–82.8; VB ≈ 0.066–0.080 mm), indicating that the highest austenitizing temperature consistently produces a tool state that suppresses flank wear. In contrast, the 800–900°C conditions show lower hardness (≈67–71 HRC) and higher VB, indicating that wear performance improves strongly with increasing temperature. Within a given temperature range, the quenching medium introduces secondary shifts in VB, with oil quenching yielding slightly lower wear than salt water at 800–900°C [28] [29]. Overall, the scatter plot supports the heatmap-based mapping outcome by confirming that the most favorable performance region corresponds to the combination of elevated hardness and reduced flank wear at 1000°C, while also highlighting that hardness alone does not fully eliminate medium-dependent differences at lower temperatures.

3.5 Composite decision mapping and condition ranking

To translate the dual objective—minimize VB and maximize HRC—into a transparent ranking, a desirability-style composite index D was evaluated using min–max normalization and equal weighting. Based on the computed mean HRC from raw readings, the highest-ranked conditions are all located at 1000°C, with the order: (1) 1000°C + SAE 20 oil: VB = 0.066 mm, HRC ≈ 82.8, D = 1.000; (2) 1000°C + Bromus oil: VB = 0.073 mm, HRC ≈ 82.2, D ≈ 0.968; (3) 1000°C + Salt water: VB = 0.080 mm, HRC ≈ 81.5, D ≈ 0.934

At 900°C, Bromus oil achieves the best combined performance among the three media (VB = 0.120 mm, HRC ≈ 71.2, D ≈ 0.452), while 800°C conditions produce the lowest scores due to higher VB.

Fig. 3 translates the dual objective of minimizing flank wear (VB) and maximizing hardness (HRC) into a single decision-oriented metric. The highest composite scores are concentrated at 1000°C, indicating that this temperature level provides the most favorable combined wear–hardness performance across all quenching media. Among the nine conditions, 1000°C with SAE 20 oil achieves the maximum score ($D = 1.000$), reflecting the lowest VB and the highest HRC in the dataset, while 1000°C with Bromus oil and 1000°C with salt water follow closely. At 900°C, composite performance improves relative to 800°C but remains clearly separated from the 1000°C region, showing that medium selection alone cannot compensate for the wear penalty at lower austenitizing temperatures. Overall, the decision map provides a transparent ranking of quenching conditions and confirms that the optimal operating region for this dataset lies at high austenitizing temperature with oil quenching, consistent with the trends observed in the VB heatmap and the VB–HRC scatter plot.

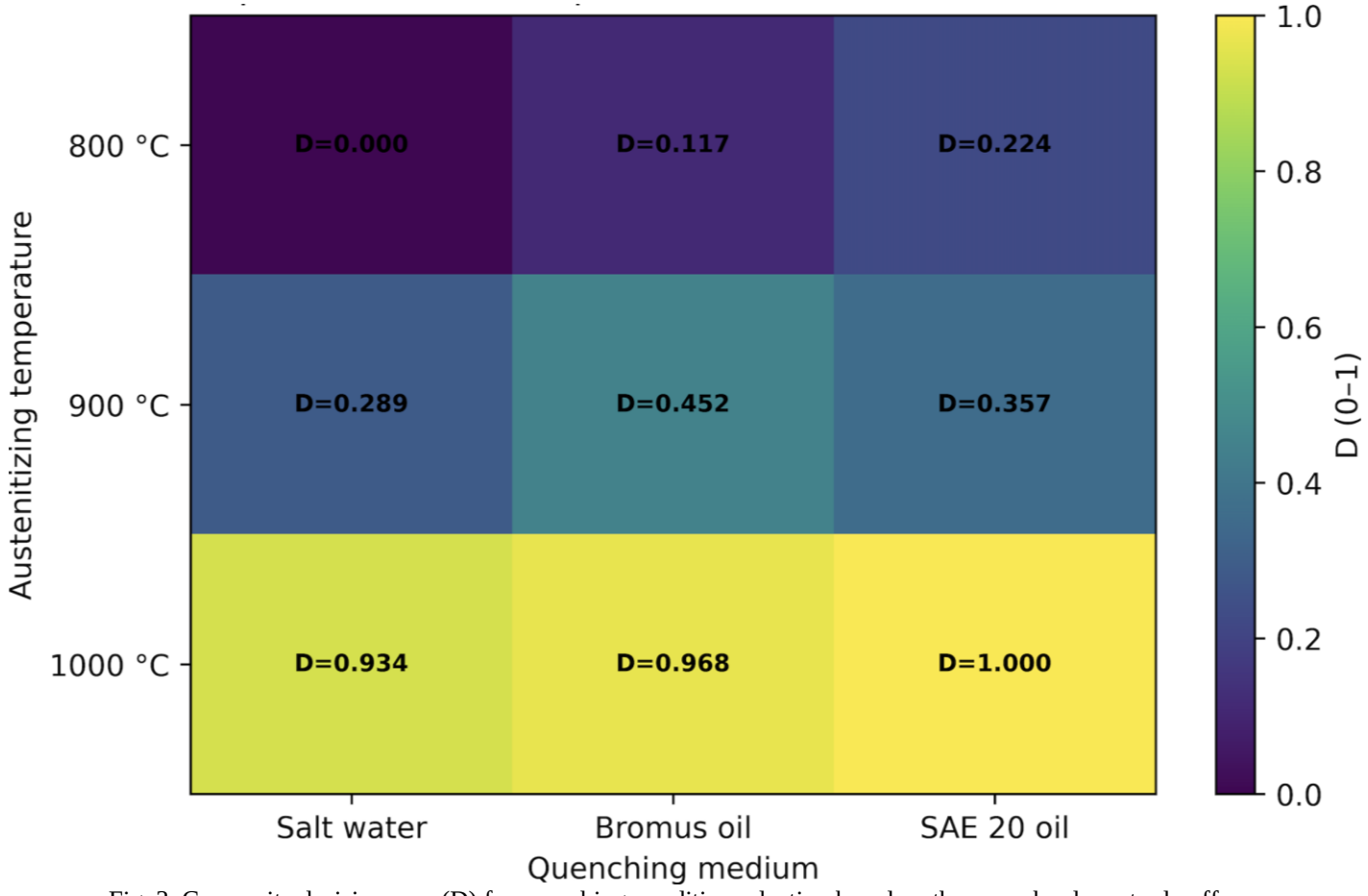

Fig. 3. Composite decision map (D) for quenching-condition selection based on the wear–hardness trade-off.

3.6 Practical implications and limitations

Under the fixed turning parameters, the results indicate that austenitizing at 1000°C yields the most favorable region for minimizing VB and maximizing the combined performance index. Within this region, SAE 20 oil provides the best overall outcome, while Bromus oil and salt water at 1000°C remain competitive because the VB values are closely grouped (0.066–0.080 mm). At 800–900°C, oil quenching consistently results in lower VB than salt water, suggesting that oil-based media are preferable when high-temperature austenitizing is not feasible. The dataset reflects one set of turning conditions and does not include additional cutting parameters (speed/feed/depth variations), full tool-life curves, or direct microstructural characterization. Therefore, the conclusions should be interpreted as valid for the tested operating window and the reported metrics (VB and HRC). Hardness values were processed using repeated measurements ($N = 5$) to support repeatability-aware interpretation. Future work may extend the mapping to additional cutting regimes and incorporate microstructural evidence to strengthen mechanistic interpretation (Fig. 4).

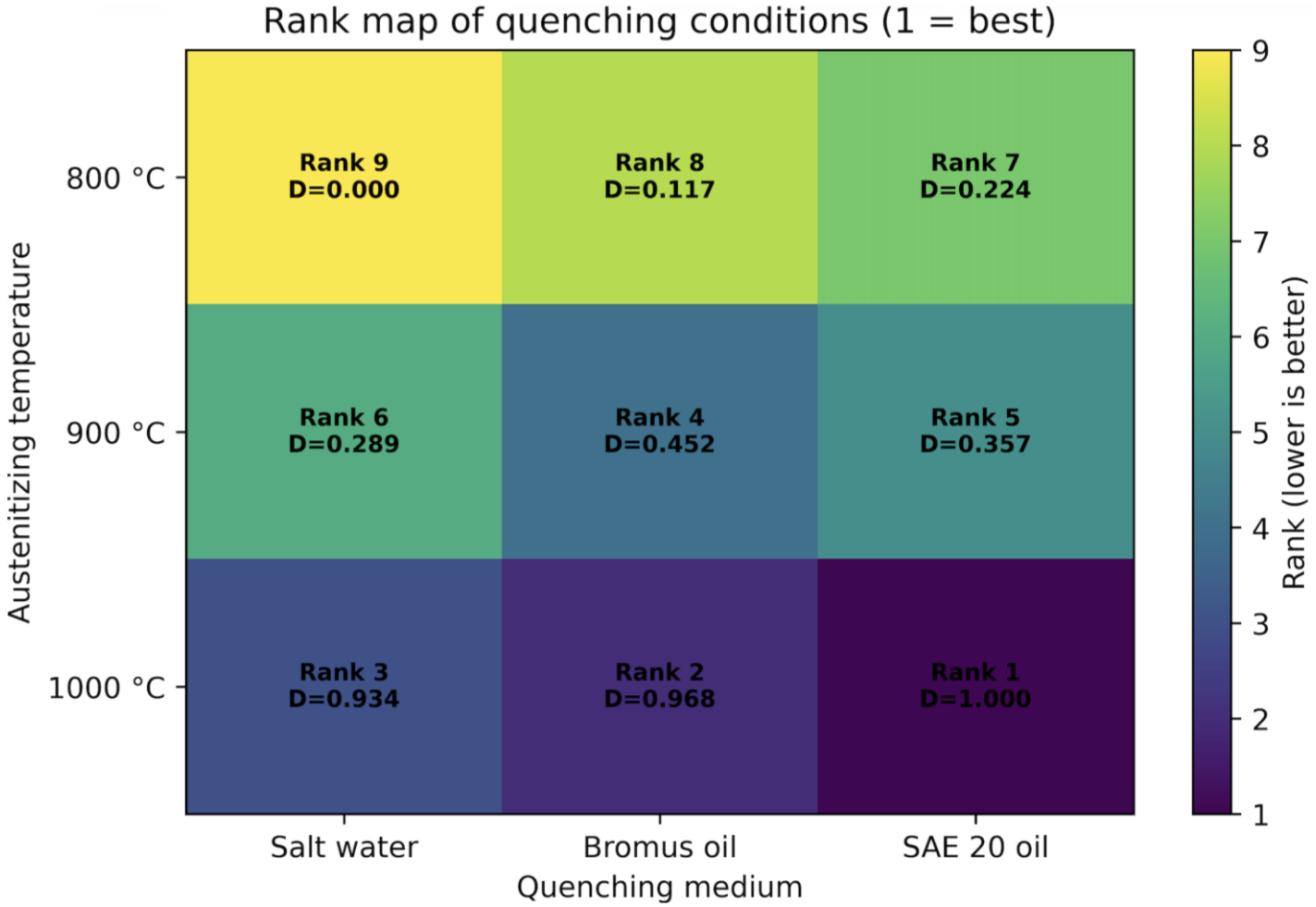

Fig. 4. Rank map (1 = best) derived from the composite index D.

4 Conclusions

This study proposed a heatmap-based wear–hardness trade-off mapping framework to evaluate quenching conditions for HSS cutting tools under fixed turning parameters (n = 300 rpm, f = 0.19 mm/rev, and a_p = 1.5 mm). By integrating flank wear (VB) and Rockwell hardness (HRC) into aligned performance maps, repeatability metrics, and a composite decision index, the study provides a compact and transparent, decision-oriented method for comparing nine temperature–medium combinations. In this sense, the main contribution of the present work is methodological, namely the development of an interpretable mapping framework for engineering selection within a small factorial heat-treatment dataset.

Across all quenching media, austenitizing temperature was identified as the dominant factor controlling tool performance. VB decreased consistently from 800°C to 1000°C, while HRC increased markedly at 1000°C, producing the most favorable wear–hardness region. Statistical validation using two-way ANOVA confirmed that austenitizing temperature had a highly significant effect on HRC, whereas the quenching medium and interaction effects were not statistically significant. This indicates that hardness is primarily governed by thermal input rather than medium-specific interactions.

From a metallurgical perspective, improved performance at higher temperature reflects more complete austenitization, leading to harder transformed structures and improved wear resistance. The best condition was 1000°C with SAE 20 oil, yielding VB = 0.066 mm and HRC ≈ 82.8. However, conclusions are limited to the tested conditions; future work should include replicated wear data, broader cutting regimes, and microstructural characterization.

References

[1] J. L. Dossett and G. E. Totten, Eds., ASM Handbook, Volume 4A: Steel Heat Treating Fundamentals and Processes. Materials Park, OH, USA: ASM International, 2013.

[2] G. A. Roberts, G. Krauss, and R. Kennedy, Tool Steels, 5th ed. Materials Park, OH, USA: ASM International, 1998.

[3] I. Hutchings and P. Shipway, Tribology: Friction and Wear of Engineering Materials, 2nd ed. Oxford, UK: Butterworth-Heinemann, 2017.

[4] J. Derringer and R. Suich, "Simultaneous Optimization of Several Response Variables," J. Qual. Technol., vol. 12, no. 4, pp. 214–219, 1980, doi: 10.1080/00224065.1980.11980968.

[5] C. Luo, Z. Huang, Z. Gao, L. Wang, M. Xiao, and Y. Zhao, "Effects of Austenitizing Conditions on the Microstructure and Mechanical Properties of High-Speed Steel," Metals, vol. 7, no. 1, p. 27, 2017, doi: 10.3390/met7010027.

[6] H. Zapata, M. R. Buitrago, and J. J. Coronado, "Wear and thermal behaviour of M2 high-speed steel, completely and partially quenched," J. Mater. Sci., vol. 33, pp. 3219–3225, 1998, doi: 10.1023/A:1004324729342.

[7] E. Fu, G. E. Totten, and J. Dossett, "The Effects of Tempering on the Toughness of an As-Cast High-Speed Steel Work Roll," J. Mater. Eng. Perform., vol. 17, pp. 535–542, 2008, doi: 10.1007/s11665-007-9174-4.

[8] J. H. Kang and Y. K. Lee, "Microstructure and Wear Resistance of High-Speed Steel Roll," Metall. Mater. Trans. A, vol. 47, pp. 3365–3374, 2016, doi: 10.1007/s11661-016-3536-1.

[9] Y. Zhou, F. Xiong, J. Xu, C. Wang, Y. Jiang, and Z. Fan, "Morphology and Properties of M2C Eutectic Carbides in AISI M2 Steel," ISIJ Int., vol. 50, pp. 1151–1157, 2010, doi: 10.2355/isijinternational.50.1151.

[10] K. C. Hwang, S. Lee, and H. C. Lee, "Effects of alloying elements on microstructure and fracture properties of cast high speed steel rolls. Part I: Microstructural analysis," Mater. Sci. Eng. A, vol. 254, pp. 282–295, 1998, doi: 10.1016/S0921-5093(98)00626-1.

[11] E. Gordo, J. M. Torralba, and R. Velasco, "Wear mechanisms in high-speed steels reinforced with NbC/TaC," Wear, vol.

239, pp. 251–259, 2000, doi: 10.1016/S0043-1648(00)00329-X.
[12] M. X. Wei, Y. T. Luo, F. Wang, and K. M. Chen, "Effects of carbon and vanadium on microstructures and abrasive wear resistance of high speed steel," Tribol. Int., vol. 39, pp. 641–648, 2006, doi: 10.1016/j.triboint.2005.04.035.
[13] Z. Zalisz, S. Zalisz, J. Kusiński, M. Rozmus-Górnikowska, L. Stobierski, and J. Borysiuk, "Friction and wear of lubricated M3 Class 2 sintered high speed steel with additions of (NbC and TaC) and VC," Wear, vol. 258, pp. 701–711, 2005, doi: 10.1016/j.wear.2004.09.069.
[14] V. B. Baglyuk and L. A. Poznyak, "Ultradispersed composition of secondary hardening of high-speed steel," Powder Metall. Met. Ceram., vol. 41, pp. 366–368, 2002, doi: 10.1023/A:1021113025628.
[15] A. Akhbarizadeh, H. Saghafian, and G. Shafyei, "Effects of cryogenic treatment on wear behavior of D6 tool steel," Mater. Des., vol. 30, no. 8, pp. 3259–3264, 2009, doi: 10.1016/j.matdes.2008.11.016.
[16] A. Akhbarizadeh, K. Amini, and S. Javadpour, "Effects of applying an external magnetic field during the deep cryogenic heat treatment on the corrosion resistance and wear behavior of 1.2080 tool steel," Mater. Des., vol. 41, pp. 114–123, 2012, doi: 10.1016/j.matdes.2012.03.045.
[17] A. Molinari, M. Pellizzari, S. Gialanella, G. Straffelini, and K. H. Stiasny, "Effect of deep cryogenic treatment on the mechanical properties of tool steels," J. Mater. Process. Technol., vol. 118, pp. 350–355, 2001, doi: 10.1016/S0924-0136(01)00973-6.
[18] J. Y. Huang, Y. T. Zhu, X. Z. Liao, I. J. Beyerlein, M. A. Bourke, and T. E. Mitchell, "Microstructure of cryogenic treated M2 tool steel," Mater. Sci. Eng. A, vol. 339, pp. 241–244, 2003, doi: 10.1016/S0921-5093(02)00165-X.
[19] D. C. Montgomery, Design and Analysis of Experiments, 10th ed. Hoboken, NJ, USA: Wiley, 2019.
[20] G. Derringer and R. Suich, "Simultaneous optimization of several response variables," Journal of Quality Technology, vol. 12, no. 4, pp. 214–219, 1980, doi: 10.1080/00224065.1980.11980968.
[21] S. J. S. Chelladurai, K. Murugan, A. P. Ray, M. Upadhyaya, V. Narasimharaj, and S. Gnanasekaran, "Optimization of process parameters using response surface methodology: A review," Materials Today: Proceedings, vol. 37, pt. 2, pp. 1301–1304, 2021, doi: 10.1016/j.matpr.2020.06.466.
[22] C. Camposeco-Negrete, "Optimization of cutting parameters using Response Surface Method for minimizing energy consumption and maximizing cutting quality in turning of AISI 6061 T6 aluminum," Journal of Cleaner Production, vol. 91, pp. 109–117, 2015, doi: 10.1016/j.jclepro.2014.12.017.
[23] R. T. Setyawan, E. Muthoriq, and S. Syahrizal, "Multi-objective tribological and energy optimization of an automatic valve lapping machine using a hybrid RSM NSGA-II approach," Jurnal Polimesin, vol. 24, no. 1, pp. 119–131, 2026, doi: 10.30811/jpl.v24i1.8454.
[24] V. K. Sharma, M. Rana, T. Singh, A. K. Singh, and K. Chattopadhyay, "Multi-response optimization of process parameters using Desirability Function Analysis during machining of EN31 steel under different machining environments," Materials Today: Proceedings, vol. 44, pp. 3121–3126, 2021, doi: 10.1016/j.matpr.2021.02.809.
[25] A. M. Rahman, S. M. A. Rob, and A. K. Srivastava, "Modeling and optimization of process parameters in face milling of Ti6Al4V alloy using Taguchi and grey relational analysis," Procedia Manufacturing, vol. 53, pp. 204–212, 2021, doi: 10.1016/j.promfg.2021.06.023.
[26] Y. Lin et al., "Multi-response optimization of process parameters in nitrogen-containing gray cast iron milling process based on application of non-dominated ranking genetic algorithm," Heliyon, vol. 8, no. 11, Art. no. e11629, 2022, doi: 10.1016/j.heliyon.2022.e11629.
[27] A. Faveto, F. Lombardi, P. Chiabert, and F. Segonds, "A circular approach to foster additive manufacturing early design stages sustainability: A methodological proposal," International Journal on Interactive Design and Manufacturing (IJIDeM), vol. 18, pp. 815–836, 2024, doi: 10.1007/s12008-023-01577-1.
[28] A. Chakrabarti, F. Ahmad, M. Jarke, and C. Quix, "Monitoring large scale production processes using a rule-based visualization recommendation system," SN Computer Science, vol. 4, Art. no. 32, 2023, doi: 10.1007/s42979-022-01419-z.
[29] Z. Sherif and K. Salonitis, "A systematic review of decision tools for process selection and performance improvement in manufacturing," The International Journal of Advanced Manufacturing Technology, vol. 141, pp. 1113–1141, 2025, doi: 10.1007/s00170-025-16806-y.